Journal of Natural Fibers

ISSN: (Print) (Online) Journal homepage: www.tandfonline.com/journals/wjnf20

Analyzing the Effects of Plasma Treatment Process Parameters on Fading of Cotton Fabrics Dyed with Two-Color Mix Dyes Using Bayesian Regulated Neural Networks (BRNNs)

Senbiao Liu, Yaohui Keane Liu, Kwan-Yu Chris Lo & Chi-Wai Kan

To cite this article: Senbiao Liu, Yaohui Keane Liu, Kwan-Yu Chris Lo & Chi-Wai Kan (2023) Analyzing the Effects of Plasma Treatment Process Parameters on Fading of Cotton Fabrics Dyed with Two-Color Mix Dyes Using Bayesian Regulated Neural Networks (BRNNs), Journal of Natural Fibers, 20:2, 2259101, DOI: 10.1080/15440478.2023.2259101

To link to this article: https://doi.org/10.1080/15440478.2023.2259101

Published online: 24 Sep 2023.

JOURNAL OF NATURAL FIBERS
2023, VOL. 20, NO. 2, 2259101
https://doi.org/10.1080/15440478.2023.2259101

Analyzing the Effects of Plasma Treatment Process Parameters on Fading of Cotton Fabrics Dyed with Two-Color Mix Dyes Using Bayesian Regulated Neural Networks (BRNNs)

Senbiao Liu[a], Yaohui Keane Liu[b], Kwan-Yu Chris Lo[a], and Chi-Wai Kan[a]

[a]School of Fashion and Textiles, The Hong Kong Polytechnic University, Kowloon, Hong Kong, China; [b]Department of Construction Technology and Engineering, Technological and Higher Education Institute of Hong Kong, Hong Kong, China

ABSTRACT

This study used Bayesian Regulated Neural Networks (BRNN) with 10-fold cross-validation to accurately forecast fading effects of plasma treatment on cotton fabrics for a given set of parameters. By training six independent BRNN models, a reduction in model complexity and an enhancement in generalizability to unknown datasets were achieved. The input comprises plasma treatment parameters and color measurements of the cotton fabric before fading, while the output comprises color measurements after fading. The plasma treatment parameters included color depth, air (oxygen) concentration, water content and treatment time. Color measurements included CIE L*a*b*C*h and K/S values. Furthermore, 162 datasets derived from two-color mixed-dye cotton fabrics were utilized for training and testing. The outcomes revealed superior prediction performance of the BRNN compared to the Levenberg-Marquardt Neural Networks, with R^2 values approaching 1 and 82.35% to 94.12% of the sample predictions lying within the acceptable color difference range. Through global sensitivity analysis, the impact of treatment parameters on fading effects was quantified, providing a scientific basis for parameter adjustment. This study not only elucidated the mechanism of plasma treatment-induced fading but also offers effective prediction tools for the intelligent and digital development of the fashion clothing fading domain.

摘要

本研究使用具有10倍交叉验证的贝叶斯调节神经网络（BRNN）来准确预测给定参数下等离子体处理对棉织物的褪色效果. 通过训练六个独立的BRNN模型，降低了模型的复杂性，增强了对未知数据集的可推广性. 输入包括等离子体处理参数和褪色前棉织物的颜色测量，而输出包括褪色后的颜色测量. 等离子体处理参数包括颜色深度、空气（氧气）浓度、含水量和处理时间. 颜色测量包括CIE L*a*b*C*h和K/S值. 此外，还利用162个来自双色混染棉织物的数据集进行训练和测试. 结果显示，与Levenberg-Marquardt神经网络相比，BRNN的预测性能优越，R2值接近1，82.35%至94.12%的样本预测处于可接受的色差范围内. 通过全局灵敏度分析，量化了处理参数对衰落效应的影响，为参数调整提供了科学依据. 这项研究不仅阐明了等离子体处理引起的褪色机制，而且为时尚服装褪色领域的智能化和数字化发展提供了有效的预测工具.

KEYWORDS

Bayesian regulated neural network; 10-fold cross-validation; sensitivity analysis; plasma treatment; two-color mix dye; fading effect prediction

关键词

贝叶斯调节神经网络; 10倍交叉验证; 灵敏度分析; 等离子体处理; 双色混合染料; 衰落效应预测

CONTACT Chi-Wai Kan tccwk@polyu.edu.hk School of Fashion and Textiles, The Hong Kong Polytechnic University, Hung Hom, Kowloon, Hong Kong, China

Introduction

A prevailing trend in fashionable clothing involves the fading of textiles to enhance their visual appeal, traditionally achieved through chemical or mechanical processes. However, these methods present challenges concerning (1) measurement precision, (2) environmental harm, and (3) difficulty in meeting high production demands (Ibrahim and Eid 2020; Liu et al. 2019; Samanta, Basak, and Chattopadhyay 2017). Plasma treatment emerges as a sustainable alternative, achieving zero emissions and improved hydrophilicity of treated textiles (Ibrahim et al. 2010; Paul 2015). It can also generate fading effects and modify surface characteristics on cotton textiles without impacting their bulk properties (Atav et al. 2022; Ibrahim et al. 2022; Kan, Cheung, and Kooh 2017). Moreover, plasma-induced ozone treatment presents high efficiency in terms of energy use, obviating the need for water or chemicals (Srikrishnan and Jyoshitaa 2022). The process of fading cotton textiles exposed to plasma-induced ozone can be represented by twelve equations, as shown in Table 1. When operating parameters for plasma treatment are kept constant, investing some effort in process optimization ensures maximum performance, uniformity, and repeatability of the plasma surface treatment process, thus achieving control over the fading effect (Peran and Ercegović Ražić 2020).

Besides, Eyupoglu, et al. (2022) demonstrated that pre-treatment with oxygen plasma can substantially enhance the wrinkle resistance and tensile strength of cellulose acetate-based textiles. Furthermore, plasma treatment with gases such as oxygen and nitrogen can improve the absorption rate and colorfastness of silk fabrics to natural dyes (Dayioglu et al. 2015; Dayioğlu et al. 2016). The dye-absorption capabilities of polyester/viscose nonwoven fabric can also be enhanced post-plasma treatment (Canbolat, Kilinc, and Kut 2015). Domonkos and Tichá (2023) spotlighted the potential of low-temperature atmospheric pressure plasma technique for its cost-effectiveness, safety, and environmental friendliness. This technique can increase the surface energy of materials and boost their adhesion, chemical alterations, printability, and dyeability (Domonkos and Tichá 2023). Haque and Naebe (2023) proposed a novel technique of plasma-assisted spray dyeing on wool, characterized by its energy efficiency, absence of wastewater, and high color intensity and colorfastness.

However, the interaction between plasma and fabric constitutes a complex process, influenced by an array of factors such as the parameters of plasma treatment, the gas used for plasma generation, and the chemical composition of the fabric (Jelil 2015; Zille, Oliveira, and Souto 2015). Critical parameters incorporate air concentration, treatment duration, and fabric moisture content (Kan, Cheung, and Chan 2016). (1) An increase in air concentration engenders more hydroxyl radicals, which, in the presence of dye, intensifies oxidation and fading (Kan, Cheung, and Chan 2016). (2) Prolonged treatment duration likewise enhances the likelihood of dye oxidation and fading (Kan, Cheung, and Chan 2016). (3) Lower water content in the fabric might augment fading, as a higher water content could dilute the bleaching agent in the plasma-induced ozone treatment process, thereby diminishing the fading effect (Kan, Cheung, and Chan 2016). Thus, to identify the optimal plasma treatment parameters for achieving the desired fading effect, iterative experimentation and observation are requisite.

In the realm of modeling complex datasets, neural networks have demonstrated superior performance over statistical models, particularly non-linear multidimensional functions, as they obviate the need for a detailed investigation of the chemical or physical characteristics of the pertinent processes (Gadekar and Ahammed 2019). For instance, the Levenberg-Marquardt Neural Network (LMNN) model, which optimizes network weights to minimize the sum of squares of errors between predicted and actual outputs, has been employed to forecast the ultraviolet protection performance of the polyester fabric and the dyeability of mohair fibers (Eyupoglu, Eyupoglu, and Merdan 2021, 2022). Additionally, certain neural networks utilize the Bayesian Regularization algorithm. This algorithm, grounded in Bayesian learning theory, introduces a priori distribution to reduce model complexity and prevent overfitting, thereby providing robust models (Kayri 2016). Notably, the fusion of plasma treatment with intelligent techniques such as Bayesian Regularized Neural Network (BRNN) can render cotton processing more sustainable by predicting fading effects, thereby reducing trial and error.

Table 1. The process of how cotton fabrics fade when exposed to plasma-induced ozone.

Descriptions	Equations	No.	References
• The first step is the release of high-energy electrons through electron impact due to plasma treatment. • Mixed radicals are produced when electrons with high energy interact with air moisture. • This process can be explained by Equation (1).	$5H_2O \xrightarrow{e^-} \cdot 2OH + e^-_{aq} + \cdot H + H_2O_2 + H_3^+O + H_2$	(1)	(Cheung 2018; Kan, Cheung, and Chan 2016, Zhang et al. 2008; Srikrishnan and Jyoshitaa 2022)
• Meanwhile, some electrons with a high energy level interact with oxygen molecules in the air. During this reaction, $O\cdot$ and O_3 are formed. • Equations (2) and (3) describe this process.	$O_2 + O\cdot \rightarrow O_3$ $O_2 \xrightarrow{e^-} 2O\cdot \xrightarrow{H_2O} 2 \cdot OH$	(2) (3)	
• Besides, it is possible to introduce ozone into the water. When injected into the water, ozone can be held for between three and twenty minutes. • As ozone is highly soluble in water, ozone produced previously is easily absorbed by airborne moisture, which serves as a powerful oxidant. • It has been reported that the radical $\cdot OH$ formed following ozone dissolution is an important cause of color fading. • A description of this process can be found in Equations (4) to (7).	$O_3 \rightarrow O_2 + O\cdot$ $O\cdot + H^+ + e^- \rightarrow \cdot OH$ $O_3 + H_2O_2 \rightarrow \cdot OH + O_2 + HO_2\cdot$ $O_3 + HO_2\cdot \rightarrow \cdot OH + 2O_2$	(4) (5) (6) (7)	
• During ozone plasma generation, charged particles, free radicals, and ultraviolet (UV) light are produced. • Additionally, UV rays, which are produced by the plasma treatment process, are also responsible for generating $\cdot OH$ radicals. • Despite this, the efficiency of $\cdot OH$ production in water via UV is rather low, while the efficiency of the production of $\cdot OH$ radical is relatively high when ozone is present. • A description of this process can be found in Equations (8) and (9).	$O_3 + H_2O \xrightarrow{h\nu} H_2O_2 + O_2$ $H_2O_2 \xrightarrow{h\nu} 2 \cdot OH$	(8) (9)	
• Among the oxidation radicals produced during the plasma process, the hydroxyl radical $\cdot OH$ is most prevalent, mainly contributing to the degradation of dyes in textiles. • $\cdot OH$ can promote the oxidation of dye molecules (RH) to produce organic radicals $R\cdot$, capable of increasing the reaction rate and can be used to further oxidize dye molecules. • In this manner, the dyed fabric was able to achieve a fading effect. • This process is described in equations (10) to (12).	$RH + \cdot OH \rightarrow H_2O + R\cdot$ $R\cdot \rightarrow \ fragmentation\ of\ R\cdot$ $R\cdot + O_2 \rightarrow ROO\cdot$	(10) (11) (12)	

Presently, research employing intelligent techniques for plasma treatment remains scarce. In available studies, three main aspects have been investigated: (1) Feedforward neural network models were used to predict wool dyeing properties after air-vacuum plasma treatment, with regression values of around 0.95 (Omerogullari Basyigit et al. 2023); (2) using generalized regression neural networks to predict dye removal in aqueous solutions (Mitrović et al. 2020); and (3) developing adaptive neural network fuzzy inference systems to predict dye intensity (K/S) in dyed wool fabrics (Haji and Payvandy 2020). Furthermore, due to the unclear interactions between plasma and fabric surfaces, selecting appropriate plasma treatment conditions proves complex (Jelil 2015). Therefore, this study aimed to develop a BRNN system to precisely predict the fading effects of plasma treatment on reactive dyed cotton fabric. To assess model accuracy and performance, five metrics were utilized: Mean Absolute Error (MAE), Root Mean Square Error (RMSE), Mean Absolute Percentage Error (MAPE), Coefficient of Determination (R^2), and running time. Besides, a global sensitivity analysis was conducted to systematically study the impact of various parameters during plasma treatment.

Methodology

Fabric samples and dyeing

Cotton single knitted fabric (Lacoste: 32s/2) with a weight of 220 g/m^2 was dyed by mixing two reactive dyes of three primary colors, red (Levafix Red CA), blue (Levafix Blue CA) and yellow (Levafix Yellow CA) at a dyeing plant in China. The dyes were supplied by DyStar, China and were used as received for dyeing without purification. Di-chloro quinoxaline is the structure of the Levafix series (Shaffer et al. 2012), as shown in Figure 1. This type of dye exhibits good lightfastness in lighter shades and excellent perspiration and lightfastness in the color range and has a high degree of reproducibility and level-dyeing properties (Cheung 2018).

Three mixed secondary colors of nacarat (RN), green (RG) and violet (RV) were used for dyeing to different depths of 0.5%, 1.5% and 3%. The dyed fabric samples were of size approximately 30 cm x 40 cm. Of these, nacarat (a shade of pale red-orange) at 0.5% concentration is made by combining dyes of equal concentrations of red and yellow. Green is made by combining equal concentrations of blue and yellow, and violet is made by combining equal concentrations of red and blue dyes. For example, in this study, a 0.5% concentration of violet is a combination of 0.5% concentration of red with a 0.5% concentration of blue, and so on. The process of dyeing cotton fabrics with dyestuff was described in Table 2 and Figure 2.

Plasma treatment of faded colors

For the plasma treatment used for fading, a commercial ozone plasma machine G2 (standard model, Spain Jeanologia) was used. In comparison to conventional processes, the G2 plasma machine saves 62% of energy (kW/h), 67% of water, 85% of chemicals, and reduces the amount of time required for production by 85% (Kan, Cheung, and Chan 2016). Using electric currents to ionize oxygen molecules within the incoming air, the G2 creates a mixture of reactive oxygen to fade textiles (Kan, Cheung, and Chan 2016). Before being returned to the atmosphere, residual ozone plasma undergoes a transformation into purified air (Kan, Cheung, and Chan 2016). Table 3 demonstrates how the specifications of G2 plasma machine.

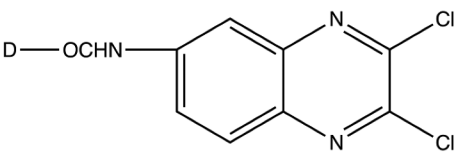

Figure 1. The dye structure about Di-chloro quinoxaline (Shaffer et al. 2012).

Table 2. The process of dyeing with reactive dyes.

Procedure of reactive dyeing	The dyeing process	References
Stage 1	(1) Dyeing of cotton fabric with 1.5% (by weight of fabric) of reactive dyestuff in a 10:1 liquid-to-goods ratio, if cotton fabric with a weight of 10 kg was to be dyed on an industry-scale winch dyeing machine. Then 42.5 g/l of salt (sodium chloride) and the cotton fabric samples were placed in a dye bath set at 30°C and treated for 10 minutes. (2) The reactive dye was then added to the dye bath within 20 minutes. (3) Salt, dye, and fabric were treated in the dye bath for a further 10 minutes. (4) Soda ash (11.5 g/L) was added to the dye bath within 15–30 minutes. (5) The fabric was then treated for a further 10 minutes.	(Cheung 2018; Kan, Cheung, and Chan 2016)
Stage 2	Temperature of the dye bath was increased to 60°C at a rate of 1°C/min within 30 minutes.	
Stage 3	After the temperature had reached 60°C, the fabric was kept in the dye bath for 60 minutes.	
Stage 4	(1) The fabric was taken from the dye bath and was rinsed under cold water so as to wash away the undyed dye. (2) Post-treatment was carried out to further remove undyed dyestuff by using a nonionic detergent with a concentration of 1.0%. (3) After the detergent treatment, the fabric was rinsed in cold water. The dyed fabric was conditioned at 20 ± 2°C and 65 ± 2% relative humidity for at least 24 hours in advance of further treatment.	

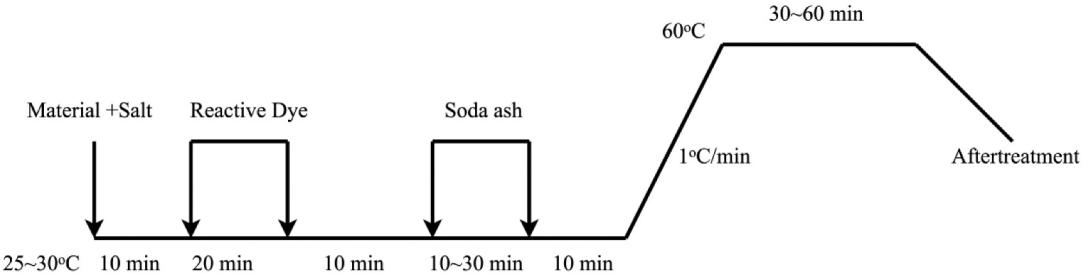

Figure 2. Procedure of reactive dyeing (Cheung 2018; Kan, Cheung, and Chan 2016).

Table 3. Technical specifications of G2 plasma machine (Cheung 2018).

Electricity power demand	9 kw per hour
Ozone plasma gas concentration	0–180 g/Nm3
Ozone plasma generator power	400 g per hour
Machine loading capacity	50 kg
50 kg convert to garments	80–100 denim jeans or 160 knitted t-shirts
Tumbler measurement	1200 1600 m/m

Table 4. Plasma treatment parameters applied to two-color mixed dyed fabric samples.

Air (Oxygen) concentration (%)	10, 30, 50
Water Content (%)	35, 45
Treatment time (minutes)	10, 20, 30

Table 4 summarizes the plasma treatment parameters used at a garment processing factory in China for cotton fabrics. Three parameters were used in the process, air concentration, dyed fabric water content and treatment time. Though 30 minutes is a long time for textile treatment, different plasma operating parameters need to be investigated to determine how fading occurs on two-color mixed dyed cotton fabrics. Different colors fade at different rates. For example, yellow fades more

slowly than blue (Atav et al. 2022). Furthermore, the operating parameters of the three plasma treatments are interdependent (Kan, Cheung, and Chan 2016). Depending on the operating parameters of the other two plasma treatments, such as providing a lower concentration of air (oxygen) and a higher water content, the treatment time of the plasma used for fading might need to be extended (Ibrahim et al. 2010; Kan, Cheung, and Chan 2016). Thus, to include the full range of acceptable plasma operating parameters, the treatment time included 30 minutes. For each type of dye, 54 fabric samples were used for color measurements, and 162 samples were used for the three different reactive dye colors. There were 18 combinations of plasma treatment parameters ($3\times3\times2=18$), and dyes were applied at three different dye concentrations ($18\times3=54$), and there were three different dyes ($54\times3=162$). These three dyes were used to produce 162 fabric samples labeled RN1-RN54 (for nacarat color), RG1-RG54 (for green color) and RV1-RV54 (for violet color).

Color measurement arrangements

Prior to measuring color, the fabric samples were conditioned at 65 ± 2% relative humidity and 20 ± 2°C for at least 24 hours. There were three types of fabrics dyed with reactive dyes: RG, RN and RV. Colors were measured as specific CIE L*a* b*C*h and K/S values. Among them, CIE C* value and CIE h value can be calculated from the CIE a* value and the CIE b* value (Hunt and Pointer 2011). Besides, to calculate the K/S value, Equation (1), the Kubelka-Munk dyeing depth equation shown below is used (Brinkworth 1972). For each type of sample, an illuminant D65, plus a large aperture value and a 10° observer angle were used to measure color with the Macbeth Color-Eye 7000A spectrophotometer. The color-measuring device was also calibrated with black and white traps. Moreover, seven fabric samples of each type and four uniformly colored areas of each fabric sample were tested and these data were averaged to improve the accuracy of the color measurements.

$$K/S = \frac{(1-R)^2}{2*R} \tag{1}$$

Modelling, simulation and prediction using BRNN

For 162 two-color mixed dye cotton fabric samples, the CIE L*a*b*C*h and K/S values were measured. After preliminary data processing, the relationship between plasma treatment process parameters and CIE L*a*b*C*h and K/S values was investigated using BRNN. 145 of these data sets were used for BRNN modeling and simulation, while the remaining 17 unseen data, selected by stratified sampling, were used for testing the generalizability of the BRNN. Table 5 below illustrates how these data sets were divided.

For the purpose of implementing regression analysis on smaller data sets, a small three-layer neural network was constructed. Utilization of the Bayesian Regularization Algorithm (BRA) was embraced to mitigate the risk of overfitting (Doan and Liong 2004). Despite the increment in processing time, the algorithm bolstered the model's generalizability (Doan and Liong 2004). Further, a 10-fold cross-validation procedure was incorporated into the model. Cross-validation is based on data division, where the majority of the data is used to train the model and the remaining small portion of the data is used to validate the error to measure the predictive performance of the model and to select the best-performing model at the end (Yadav and Shukla 2016; Zhang and Yang 2015). For each training

Table 5. Division of the data sets.

Datasets for training and validation (145)	Unseen datasets of BRNN for testing (17)
RG1, RG3-RG11, RG13-RG21, RG23-RG31, RG33-RG41, RG43-RG51, RG53, RG54	RG2, RG12, RG22, RG32, RG42, RG52
RN1-RN7, RN9-RN17, RN19-RN27, RN29-RN37, RN39-RN47, RN49-RN54	RN8, RN18, RN28, RN38, RN48
RV1-RV3, RV5-RV13, RV15-RV23, RV25-RV33, RV35-RV43, RV45-RV53	RV4, RV14, RV24, RV34, RV44, RV54

session, the data sets were divided into ten subsets, one of which is used for validation, and the other nine are used for training. There were ten repetitions of such training. Each training session has between 3 and 12 hidden layers of neurons, depending on the number of input and output layers, with the optimal number of hidden layers being determined by the particular training session. After the selected network has been trained 10 times and has met the performance target in different training rounds, the final value is calculated by taking the average of the 10 runs. In the case of limited datasets, a modular approach was further used to minimize the complexity of the neural network in addition to BRA and cross-validation (Choudhury, Berndt, and Man 2015). The designed BRNN model was divided into six modules in order to predict the six output values. Modularization facilitates the understanding of the relationship between each output value and the plasma processing parameters, thereby reducing training time at the same time. With the input and output values shown in Figure 3, six similar neural network modules were created. Furthermore, the outcomes from the Levenberg-Marquardt Neural Networks (LMNNs) will be attainable when the implemented BRA was substituted with the Levenberg-Marquardt Algorithm. A comparative analysis of the BRNNs and the LMNNs serves as an approach to scrutinize the performance of the BRNN model in greater depth.

Figure 3 illustrates that in the fading prediction system, the input consists of plasma treatment parameters as well as color measurements of the cotton fabric before fading treatment, while the output comprises color measurements after fading treatment. MATLAB (version R2021a) software was used to construct the BRNN model, with the maximum number of training epochs (iterations) set to 1000 so that the network would have sufficient time and iterations to minimize the error. For transfer functions of the hidden and output layers, MATLAB's built-in functions "logsig" and "purelin" were used respectively. Additionally, a learning rate of 0.01 was also set, as well as a training termination error of 10^{-6}. Prior to training, data normalization was undertaken to mitigate computational errors associated with parameter magnitude and to attenuate the influence of outliers (Farooq et al. 2021). Figure 4 illustrates the BRNN model's topology. In order to assess the applicability and generalizability of the BRNN model, the final BRNN model was used to predict an unseen dataset of 17 (Figure 5).

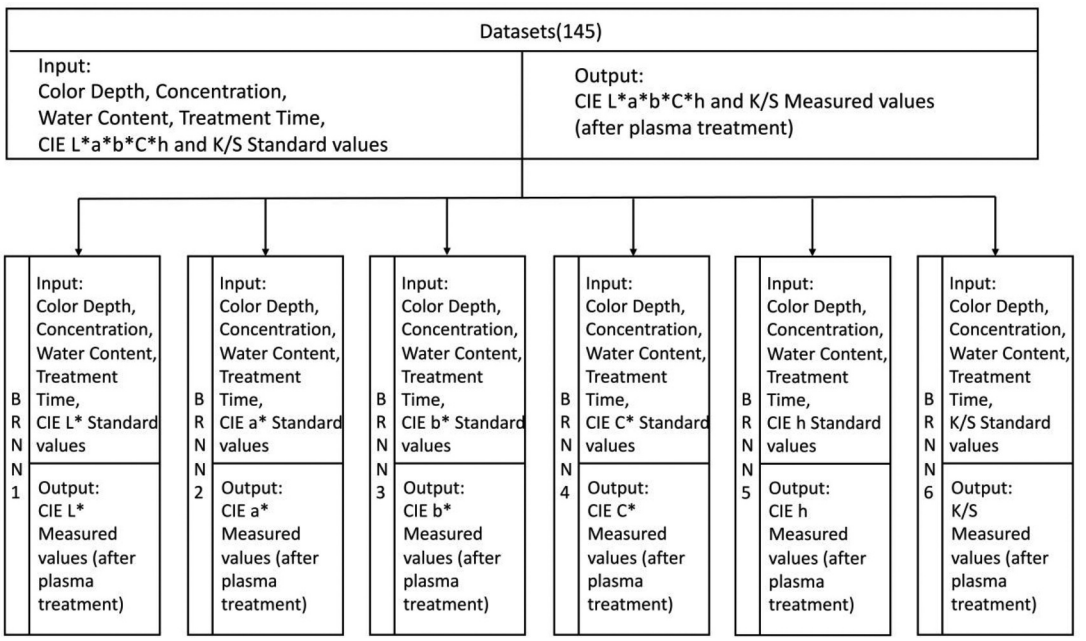

Figure 3. Six BRNN models with their inputs and outputs.

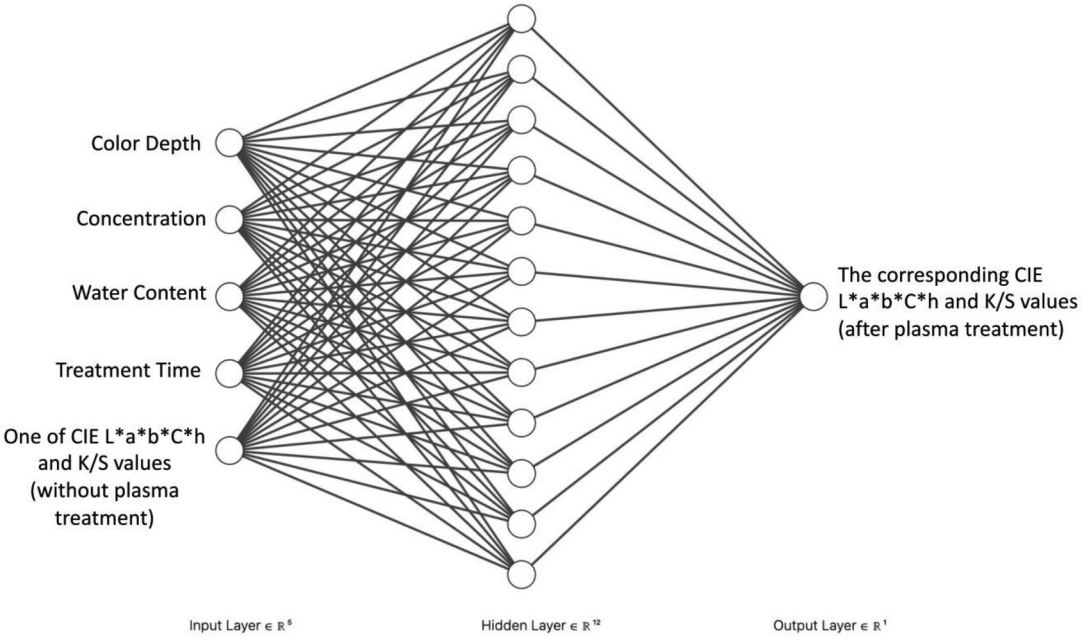

Figure 4. The topology of BRNN models.

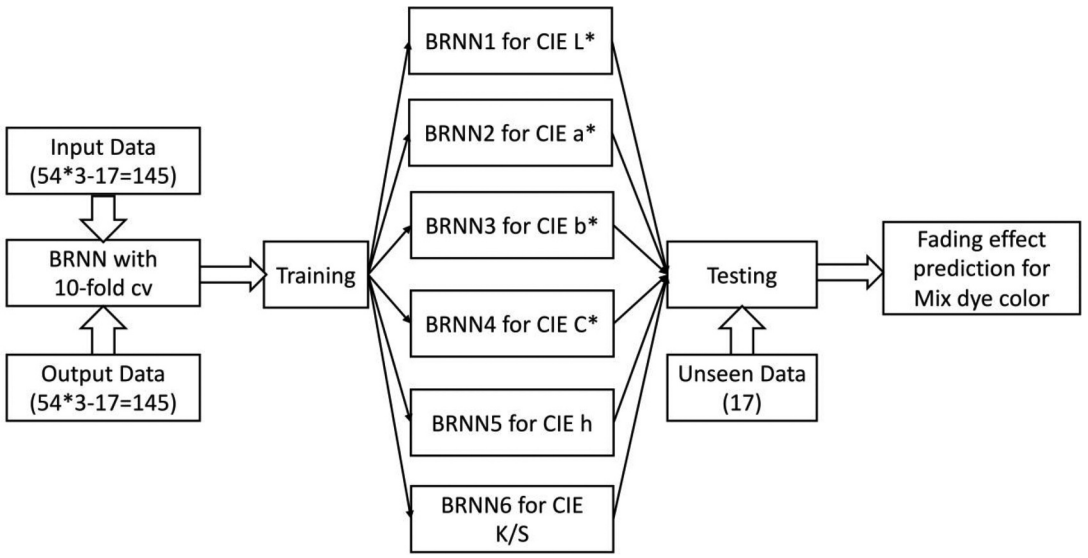

Figure 5. A flowchart showing how BRNN models predict fading effects.

Verification of the BRNN's accuracy

The evaluation of model performance typically involves a composite of metrics, including MAE, MAPE, RMSE, and R^2 (Chai and Draxler 2014). Each metric possesses inherent advantages: MAE is applicable to uniformly distributed errors, RMSE is sensitive to outliers, MAPE offers a measure of relative performance, while R^2 yields insights into a model fit (Chai and Draxler 2014; Ostertagova and Ostertag 2012). However, a single metric cannot furnish a comprehensive evaluation, for instance, R^2 lacks information regarding residuals. Consequently, a combined indicator evaluation system is more

appropriate for assessing the overall performance of the model (Chai and Draxler 2014). In addition, sensitivity analysis can be employed to rank the influence of input parameters on model outputs, with the Sobol index serving as a measure commonly utilized in the global sensitivity analysis (Iooss and Prieur 2019). The first-order Sobol index signifies the portion of total variance instigated by a singular parameter, while the total-order Sobol index represents the proportion of total variance precipitated by a parameter and all its interactions with other parameters (Iooss and Prieur 2019). If the discrepancy between the first-order and total-order Sobol indices of a parameter is minimal, it infers that the interplay among input parameters is relatively weak (Iooss and Prieur 2019). Evaluating the contribution of each parameter to the output results via global sensitivity analysis will facilitate an enhanced comprehension of the intricacies of the plasma treatment process, thus providing guidance for experimental design and parameter optimization.

Results and discussion

Table 6 exhibits the performance of BRNN and LMNN modules, with MAE, MAPE, and RMSE metrics within an acceptable range of CIE L*a*b*C* values, albeit slightly larger for CIE h and K/S values. The prediction error may be attributed to the influence of cotton fabric structure on sample reflectance at certain wavelengths, consequently affecting the K/S values. The R^2 values for CIE L*a*b*C*h are exceptionally close to 1, indicating excellent model fitting, although there exists some deviation in the predicted K/S values. Comparison between BRNN and LMNN reveals that BRNN outperforms LMNN in predicting CIE L*a*b*C*h and K/S values, exhibiting lower MAE, RMSE, and MAPE values, and higher R^2 values. However, as the training process of BRA entails employing prior distributions to estimate model hyperparameters, BRNN necessitates more running time (Kayri 2016). Despite this, the great predictive performance of BRNN justifies the tolerable reduction in computational efficiency.

Furthermore, through global sensitivity analysis, an examination was conducted concerning the impact of various parameters on fabric color during plasma treatment (Table 7). According to the Sobol indices, it was discerned that: (1) The depth of color in the fabric and the initial CIE L* value of the color significantly influenced the CIE L* after plasma treatment, accounting for 36.14% and 61.07%, respectively. (2) The initial color of the fabric primarily affected the CIE a*, CIE b*, CIE C*, and CIE h values, constituting 85% to 96%, while the influence of other input parameters remained relatively minimal. (3) Concerning the K/S value, treatment duration, initial color, air concentration, and color depth played pivotal roles, with ratios of 35.86%, 30.39%, 19.92%, and 14.35%, respectively, whereas the effect of water content could be deemed negligible (0.14%). (4) The disparity between the first-order and total-order Sobol indices of input parameters was minimal, indicating that the interaction of individual input parameters with other parameters had a relatively minor impact on the output. (5) Similar to the study conducted by Kan, Cheung, and Chan (2016), this study focused on the influence of varying parameters on fabric fading during plasma treatment, but further quantified

Table 6. Performance of the six trained BRNN and LMNN models.

	Output Values	MAE	RMSE	MAPE (%)	Coefficient of determination (R^2)	Running time (s)
BRNN1	CIE L*	0.7056	0.9476	1.1451	0.9939	82.00
LMNN1		1.2208	1.5305	2.6334	0.9835	68.17
BRNN2	CIE a*	0.5766	0.7212	4.0250	0.9989	80.22
LMNN2		0.8940	1.1282	7.9998	0.9973	69.90
BRNN3	CIE b*	0.6077	0.8257	4.5659	0.9979	81.56
LMNN3		0.9436	1.2223	6.8171	0.9951	68.33
BRNN4	CIE C*	0.6283	0.8228	2.4275	0.9963	82.95
LMNN4		1.1887	1.5217	4.8145	0.9905	69.16
BRNN5	CIE h	3.5861	7.5433	3.1745	0.9935	90.22
LMNN5		4.3377	6.8176	5.4533	0.9955	68.68
BRNN6	K/S	9.8915	14.1220	10.2545	0.9700	97.35
LMNN6		12.9822	17.6250	14.7091	0.9519	68.36

Table 7. First-order and total-order Sobol indices for different output values.

		Input parameters				
Output values	Sobol index	Color Depth	Air Concentration	Water Content	Treatment Time	One of color measurements before plasma treatment
CIE L*	First-order	0.3475	0.0031	0.0001	0.0341	0.5918
	Total-order	0.3614	0.0034	0.0031	0.0346	0.6107
CIE a*	First-order	0.0108	0.0152	0.0016	0.0175	0.9409
	Total-order	0.0142	0.0187	0.0022	0.0240	0.9514
CIE b*	First-order	0.0444	0.0001	0.0030	0.0004	0.9166
	Total-order	0.0586	0.0067	0.0034	0.0154	0.9512
CIE C*	First-order	0.0418	0.0387	0.0018	0.0567	0.8547
	Total-order	0.0432	0.0404	0.0022	0.0589	0.8574
CIE h	First-order	0.0277	0.0154	0.0023	0.0017	0.9455
	Total-order	0.0326	0.0181	0.0055	0.0039	0.9611
K/S	First-order	0.1393	0.1944	0.0012	0.3505	0.2971
	Total-order	0.1435	0.1992	0.0014	0.3586	0.3039

their impact through sensitivity analysis. For instance, the impact hierarchy on the K/S value was treatment duration (35.86%) > pre-treatment K/S value (30.39%) > color depth (14.35%) > air concentration (19.92%) > water content (0.14%). The novelty lies in the application of global sensitivity analysis to plasma treatment, offering a new perspective for textile research. By understanding the influence of each parameter on fabric color, we can better optimize the plasma treatment process, fostering its application in the textile sector.

In order to further test the utility and generalizability of trained BRNN modules, six modules were tested on 17 datasets not involved in training and validation, and the predicted values were compared to the actual values (Figures 6–11). As shown in Figures 6–10, the predicted and actual values are very close to each other, and the fitted trends are essentially the same, indicating that the model provides good predictions of CIE L*a*b*C*h values of the unseen dataset. Figure 11 depicts a similar trend, with the predicted values being slightly different from the actual results. Table 8 presents a comparison of predicted and actual values, and Equations (2) and (3) provide the formulas for calculating the difference and the MAE of ΔCIE L*a*b*C*h of predicted and actual values. The MAE of ΔCIE L*a*b*C* does not exceed 1, and the values of ΔCIE h and ΔK/S are slightly larger. Since K/S values are calculated based on the reflectance spectrum of dyed cotton fabric, they indicate the amount of dye

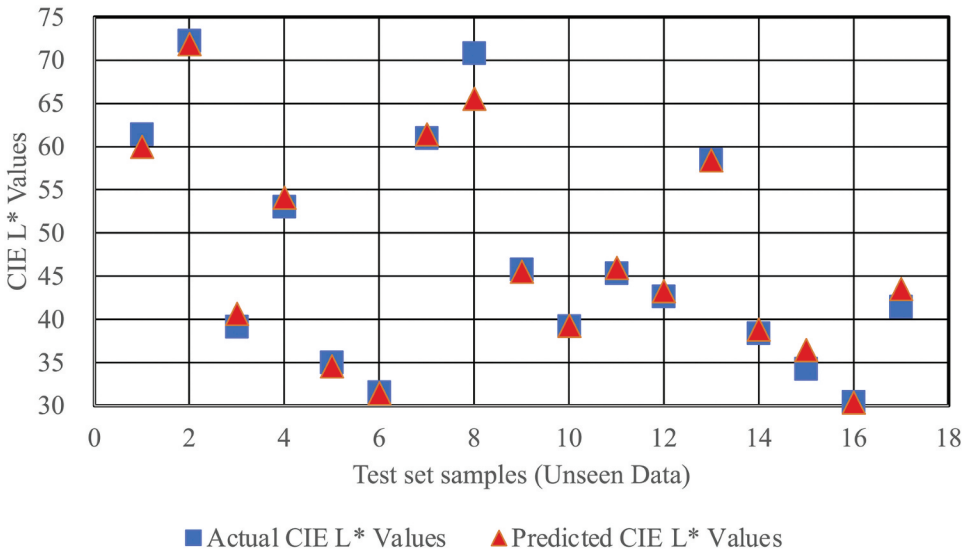

Figure 6. The predicted and actual CIE L* values in unseen data set.

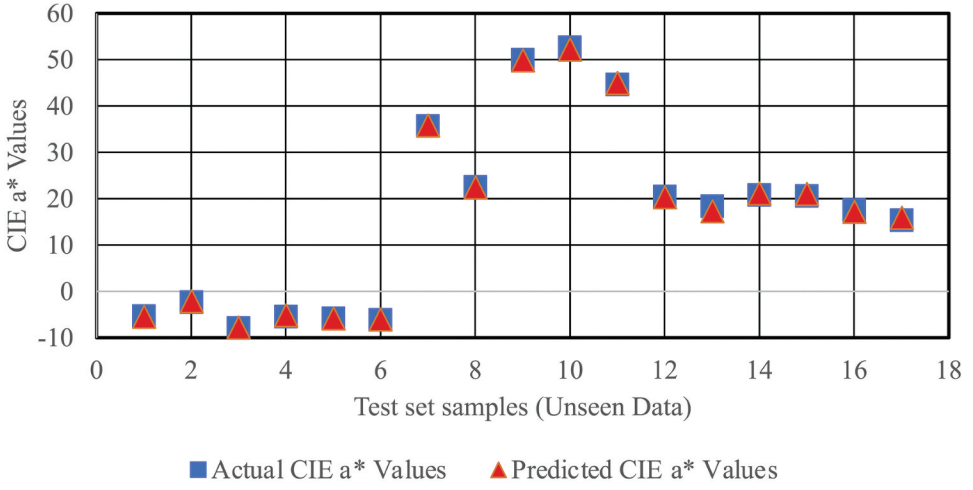

Figure 7. The predicted and actual CIE a* values in unseen data set.

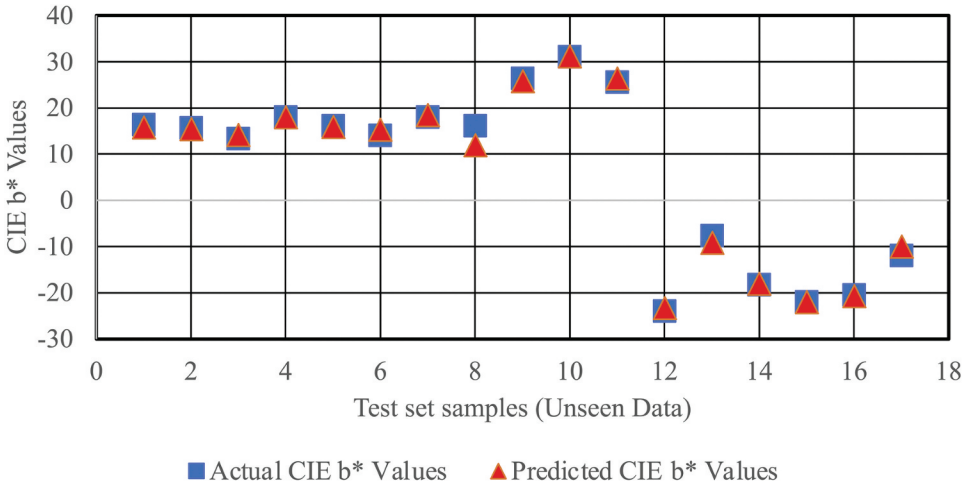

Figure 8. The predicted and actual CIE b* values in unseen data set.

present in the dyed fabric (Özkan, Baykal, and Özdemir 2018; Tang et al. 2018). The probable cause of its inaccuracy may be at the measuring stage, which is impacted by the fabric structure, texture, evenness of dyeing, and flatness (Özkan, Baykal, and Özdemir 2018). For instance, K/S values of cotton knitwear can be significantly affected by fiber structure and fabric porosity (Özkan, Baykal, and Özdemir 2018). It is possible that there is already some error in K/S values at the time of measurement, which can cause more significant errors during prediction.

$$\Delta CIE\, L^*a^*b^*C^*h\ values = Predicted\ values - Actual\ values \tag{2}$$

$$\text{The MAE of } \Delta\ CIE\, L^*a^*b^*C^*h\ or\ K/S\ values = \frac{\sum_{i=1}^{n} |\Delta\ CIE\, L^*a^*b^*C^*h\ or\ K/S\ values|}{n} \tag{3}$$

The effectiveness of the trained BRNN model was evaluated by comparing predicted and actual color values from an unknown dataset using the CMC, CIE94, and CIE2000 color difference formulas. A color difference (ΔE) of 1.0 units, deemed acceptable in the textile industry, is typically imperceptible to

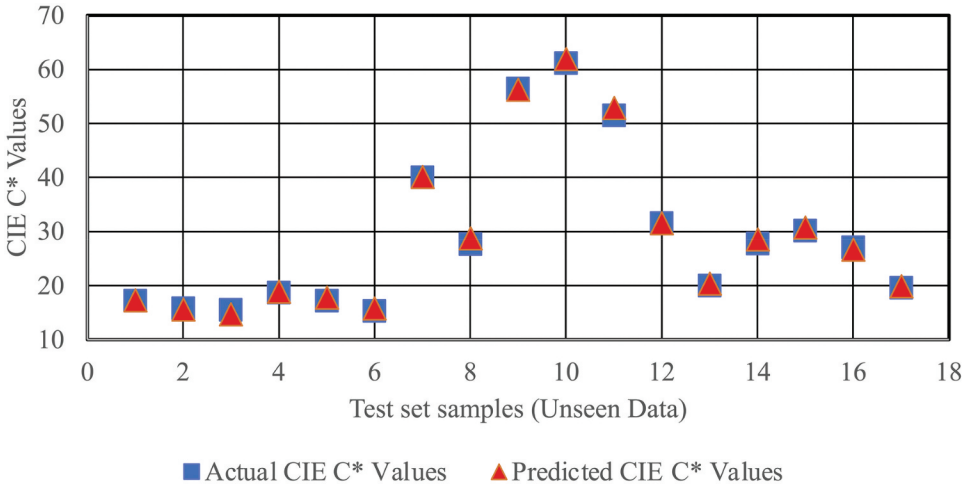

Figure 9. The predicted and actual CIE C* values in unseen data set.

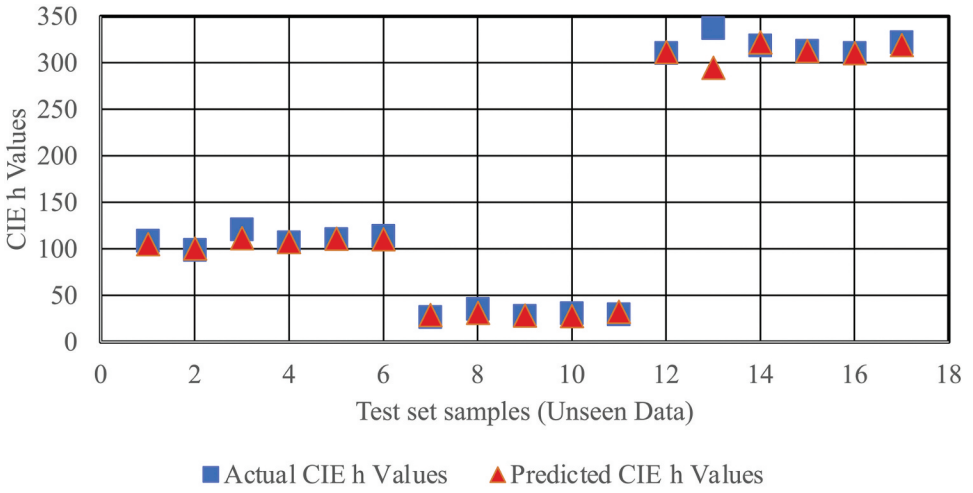

Figure 10. The predicted and actual CIE h values in unseen data set.

observers, while a ΔE between 1 and 2 is noticeable to experienced observers, and a ΔE exceeding 2 is discernible to novices (Minaker, Mason, and Chow 2021). Therefore, the tolerance value of ΔE set at 2 is acceptable. As shown in Table 9, values with superscript "*" are outside the tolerance limits (RN18, RV34 and RV54). As a result, of the 17 sets of data, between 82.35% and 94.12% of predicted colors were within the acceptable or imperceptible range based on different color differences formulas. Table 10 and Figure 12 illustrate the color differences measured by different formulas.

In general, the BRNN with 10-fold cross-validation exhibits adaptability to training datasets, generalizability to unseen data, and efficacious color difference prediction within acceptable boundaries. This underscores the repeatability and scalability of the BRNN model, not merely facilitating the fitting of known data, but also forecasting the fading effect of two-color dyed cotton fabric under various plasma treatment parameters. Nonetheless, minor predictive errors have surfaced due to deviations in color measurements, and fabric characteristics such as dye uniformity, fabric smoothness, structure, and surface texture, in conjunction with finite sample

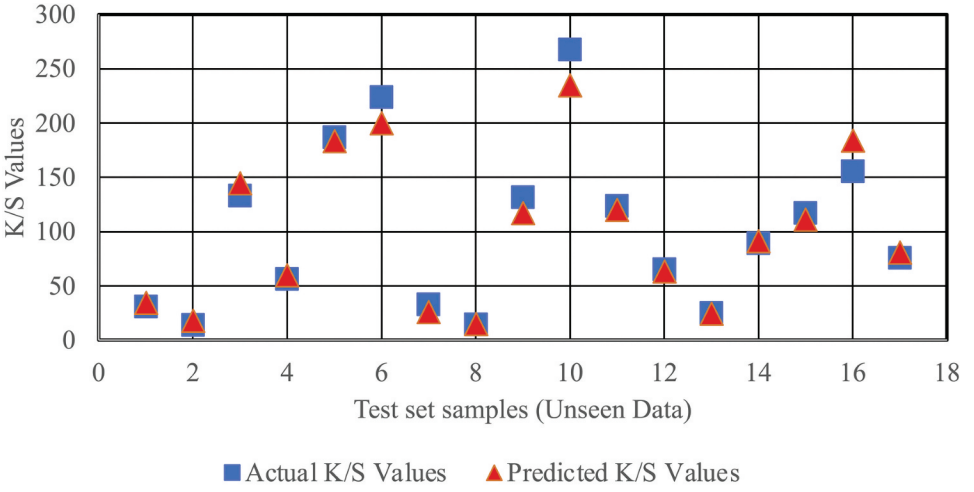

Figure 11. The predicted and actual K/S values in unseen data set.

Table 8. Difference between predicted and actual CIE L*a*b*C*h values or K/S values.

No.	ΔCIE L* values	ΔCIE a* values	ΔCIE b* values	ΔCIE C* values	ΔCIE h values	ΔK/S values
RG2	1.44	0.08	0.56	−0.11	3.43	−3.52
RG12	0.38	−0.25	0.17	0.17	−1.57	−4.23
RG22	−1.50	−0.12	−0.78	0.81	9.25	−11.17
RG32	−1.04	−0.30	−0.05	−0.15	−0.41	−3.03
RG42	0.42	−0.05	0.27	−0.58	−0.88	3.72
RG52	0.13	−0.07	−1.29	−0.47	3.23	24.19
RN8	−0.48	−0.08	−0.49	−0.18	−2.16	6.67
RN18	5.26	0.04	4.13	−1.04	4.30	−0.41
RN28	0.29	0.10	0.54	0.24	−0.74	14.02
RN38	−0.05	0.56	−0.08	−0.80	2.86	33.36
RN48	−0.62	−0.28	−0.81	−1.37	−2.73	3.59
RV4	−0.64	0.17	−0.69	0.04	−0.89	2.23
RV14	0.01	1.15	1.55	−0.37	42.83	0.08
RV24	−0.45	−0.36	−0.25	−0.82	−3.25	−1.75
RV34	−2.18	−0.57	0.06	−0.58	0.42	6.13
RV44	0.07	0.32	0.19	0.38	0.30	−28.54
RV54	−2.05	−0.56	−2.03	−0.37	2.79	−4.93
MAE	1.00	0.30	0.82	0.50	4.83	8.92

size (Özkan, Baykal, and Özdemir 2018; Tang et al. 2018). Although 10-fold cross-validation bolsters the predictive capacity for smaller datasets, due to the inherent randomness in splitting the training data, it still engenders minor inaccuracies, causing fluctuations in average precision (Fushiki 2011; Rodriguez, Perez, and Lozano 2009).

Thus, the trained and validated BRNN models can effectively reduce the number of trials required to achieve a specific color change in reactive dyed cotton fabrics after plasma treatment. Global sensitivity analysis, employing Sobol indices, delivers quantifiable insights regarding the impact of various parameters during plasma treatment on the coloration of the fabric. The adjustment of plasma treatment parameters in this manner translates to significant savings in time and resources. Future endeavors will encompass the prediction of fading effects of diverse color combinations in apparel through intelligent technology, thereby enhancing the feasibility of plasma treatment technique in fashionable attire. By simulating the fading of cotton textiles under plasma treatment using intelligent techniques, manufacturers can propel the digitalization and intellectualization of cotton processing, thus advancing the industrialization of plasma fading treatment technique.

Table 9. Color difference between predicted and actual values and color depiction figure.

No.	ΔE(CIE94)	ΔE (CMC) (1: 1)	ΔE (CIE 2000) (1:1:1)	Color depiction figure	
				Actual color	Predicted color
RG2	0.80	1.27	1.31		
RG12	0.29	0.41	0.41		
RG22	0.93	1.72	1.43		
RG32	0.58	0.99	1.07		
RG42	0.26	0.51	0.38		
RG52	0.82	1.00	0.84		
RN8	0.37	0.51	0.50		
RN18	3.76*	5.33*	5.00*		
RN28	0.30	0.41	0.39		
RN38	0.22	0.27	0.24		
RN48	0.49	0.75	0.72		
RV4	0.46	0.73	0.69		
RV14	1.49	1.52	1.35		
RV24	0.38	0.56	0.49		
RV34	1.14	2.51*	1.83		
RV44	0.28	0.29	0.31		
RV54	1.90	2.68*	2.38*		

Table 10. Summary of the color differences measured by different formulas.

Color difference formula	Average values	Minimum values	Maximum values	Passing Rate
ΔE(CIE94)	0.85	0.22	3.76	94.12% (= 16/17100%)
ΔE (CMC) (1: 1)	1.26	0.27	5.33	82.35% (= 14/17100%)
ΔE (CIE 2000) (1:1:1)	1.14	0.24	5.00	88.24%(= 15/17100%)

The number of the unseen Data is 17, the tolerance setting is 2.

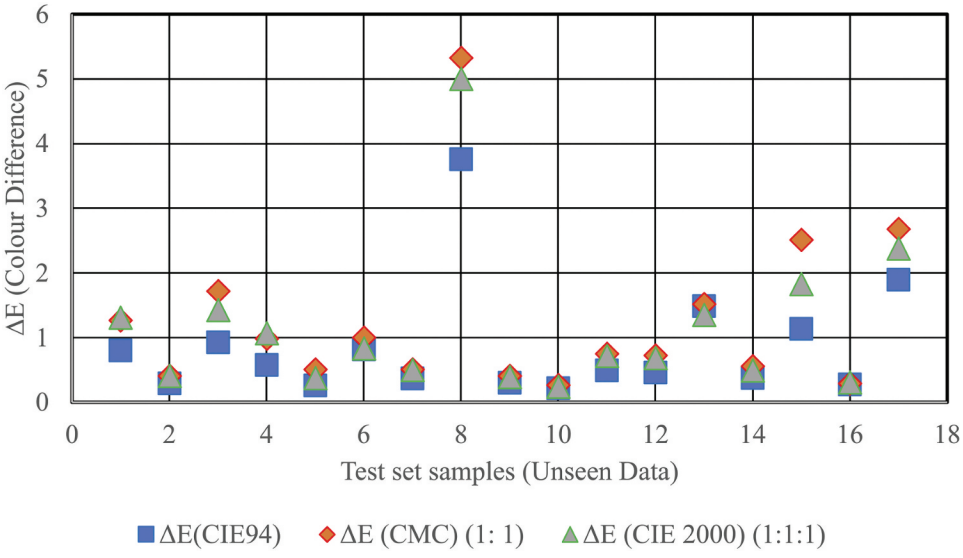

Figure 12. Color difference between the actual value and predicted value on unseen data.

Conclusions

Plasma treatment of cotton fabrics dyed with two-color mix dyes is an environmentally friendly method of fading. Six distinct BRNN modules were employed to forecast CIE L*, CIE a*, CIE b*, CIE C*, CIE h, and K/S values. The modular approach simplified the models while enhancing their versatility. The superior performance of BRNN was evident in comparison with the LMNN model. The integrated system of these models can predict the fading effect and color produced by specific plasma treatment parameters. BRNN models exhibited low and acceptable MAEs, RMSEs, and MAPEs for CIE L*a*b*C*h values, with R^2 values nearing 1 and over 82% of color predictions within an acceptable range, signifying accurate forecasting results. A global sensitivity analysis revealed and quantified the influence of treatment time, color depth, and concentration parameters on the fading effect, providing a scientific foundation for parameter adjustment and reduction of unnecessary trials. Future research will apply BRNN models to predict optimal fading effects under different plasma treatment parameters, propelling the intelligent digitization process of fashion garment fading.

Highlight

(1) The Bayesian Regularized Neural Network (BRNN) model, coupled with a modular approach and 10-fold cross-validation, enables the precise prediction of the fading effect of two-color mixed-dye cotton fabrics subjected to plasma treatment.
(2) The deployment of six independent BRNN models to predict CIE L*, CIE a*, CIE b*, CIE C*, CIE h and K/S values reduces model complexity while enhancing generalizability for unfamiliar datasets.
(3) Compared to the Levenberg-Marquardt Neural Network (LMNN) model, the BRNN generally outperforms in predicting CIE L*a*b*C*h values and K/S values. The closer R^2 values to 1 attest to the superior predictive accuracy of the BRNN model.
(4) Global sensitivity analysis elucidates and quantifies the influence of parameters such as treatment time, color depth, and concentration on the fading effect of two-color mixed-dye cotton fabrics during plasma treatment, providing a scientific basis for parameter adjustments.
(5) This research not only discloses the fading mechanism of plasma treatment but also offers an effective predictive tool for the intelligent and digital development of the fashion fading field.

Disclosure statement

No potential conflict of interest was reported by the author(s).

Funding

The work was supported by the Hong Kong Polytechnic University [ZDCC].

References

Atav, R., M. F. Yüksel, S. Özkaya, and B. Buğdaycı. 2022. The use of ozone technology for color stripping and obtaining vintage effect on reactive dyed cotton fabrics. *Journal of Natural Fibers* 19 (13):6648–58. doi:10.1080/15440478.2021.1929653.

Brinkworth, B. 1972. Interpretation of the Kubelka-Munk coefficients in reflection theory. *Applied Optics* 11 (6):1434–35. doi:10.1364/AO.11.001434.

Canbolat, S., M. Kilinc, and D. Kut. 2015. The investigation of the effects of plasma treatment on the dyeing properties of polyester/viscose nonwoven fabrics. *Procedia-Social and Behavioral Sciences* 195:2143–51. doi:10.1016/j.sbspro.2015.06.278.

Chai, T., and R. R. Draxler. 2014. Root mean square error (RMSE) or mean absolute error (MAE)?–arguments against avoiding RMSE in the literature. *Geoscientific Model Development* 7 (3):1247–50. doi:10.5194/gmd-7-1247-2014.

Cheung, H. F. C. 2018. Non-aqueous color fading effect on cotton with industrial application. Ph.D. Doctoral dissertation, Institute of Textiles and Clothing, The Hong Kong Polytechnic University.

Choudhury, T. A., C. Berndt, and Z. Man. 2015. Modular implementation of artificial neural network in predicting in-flight particle characteristics of an atmospheric plasma spray process. *Engineering Applications of Artificial Intelligence* 45:57–70. doi:10.1016/j.engappai.2015.06.015.

Dayioglu, H., D. Kut, N. Merdan, and S. Canbolat. 2015. The effect of dyeing properties of fixing agent and plasma treatment on silk fabric dyed with natural dye extract obtained from Sambucus ebulus L. plant. *Procedia-Social and Behavioral Sciences* 195:1609–17. doi:10.1016/j.sbspro.2015.06.201.

Dayioğlu, H., N. Merdan, S. Eyüpoğlu, M. Kilinc, and K. Dilek. 2016. The effect of plasma treatment on the dyeability of silk fabric by using phytolacca decandra L. natural dye extract. *Textile & Apparel* 26 (3):262–69.

Doan, C. D., and S. Y. Liong. 2004. Generalization for multilayer neural network bayesian regularization or early stopping. Proceedings of Asia Pacific association of hydrology and water resources 2nd conference, Singapore, July 5-8.

Domonkos, M., and P. Tichá. 2023. Low-temperature atmospheric pressure plasma treatment in the polymer and textile industry. *IEEE Transactions on Plasma Science*, 1–11. doi:10.1109/TPS.2023.3235266.

Eyupoglu, C., S. Eyupoglu, and N. Merdan. 2021. A multilayer perceptron artificial neural network model for estimation of ultraviolet protection properties of polyester microfiber fabric. *The Journal of the Textile Institute* 112 (9):1403–16. doi:10.1080/00405000.2020.1819000.

Eyupoglu, C., S. Eyupoglu, and N. Merdan. 2022. Investigation of dyeing properties of mohair fiber dyed with natural dyes obtained from candelariella reflexa. *Journal of Natural Fibers* 19 (16):12829–48. doi:10.1080/15440478.2022.2076273.

Eyupoglu, S., C. Karabulut, S. E. Gül, A. T. Esener, F. Yılmaz, M. Ahrari, C. Eyupoglu, and D. Kut. 2022. The effect of oxygen plasma treatment on wrinkle resistance of cellulose acetate based fabric. *Journal of Natural Fibers* 19 (17):15653–62. doi:10.1080/15440478.2022.2131686.

Farooq, A., F. Irshad, R. Azeemi, and N. Iqbal. 2021. Prognosticating the shade change after softener application using artificial neural networks. *AUTEX Research Journal* 21 (1):79–84. doi:10.2478/aut-2020-0019.

Fushiki, T. 2011. Estimation of prediction error by using K-fold cross-validation. *Statistics and Computing* 21 (2):137–46. doi:10.1007/s11222-009-9153-8.

Gadekar, M. R., and M. M. Ahammed. 2019. Modelling dye removal by adsorption onto water treatment residuals using combined response surface methodology-artificial neural network approach. *Journal of Environmental Management* 231:241–48. doi:10.1016/j.jenvman.2018.10.017.

Haji, A., and P. Payvandy. 2020. Application of ANN and ANFIS in prediction of color strength of plasma-treated wool yarns dyed with a natural colorant. *Pigment & Resin Technology* 49 (3):171–80. doi:10.1108/PRT-10-2019-0089.

Haque, A. N. M. A., and M. Naebe. 2023. Zero-water discharge and rapid natural dyeing of wool by plasma-assisted spray-dyeing. *Journal of Cleaner Production* 402:1–10. doi:10.1016/j.jclepro.2023.136807.

Hunt, R. W. G., and M. R. Pointer. 2011. Relations between colour stimuli. In *Measuring colour*, ed. M. A. Kriss, 41–57. United Kingdom: John Wiley & Sons.

Ibrahim, N. A., and B. M. Eid. 2020. Plasma treatment technology for surface modification and functionalization of cellulosic fabrics. In *Advances in functional finishing of textiles*, ed. M. Shahid and R. Adivarekar, 275–87. Singapore: Springer.

Ibrahim, N., E. El-Zairy, S. Barakat, and B. M. Eid. 2022. Eco-friendly surface modification and multifunctionalization of cotton denim fabric. *Egyptian Journal of Chemistry* 65 (13):39–51. doi:10.21608/EJCHEM.2022.147161.6382.

Ibrahim, N. A., M. M. Hashem, M. A. Eid, R. Refai, M. El-Hossamy, and B. M. Eid. 2010. Eco-friendly plasma treatment of linen-containing fabrics. *The Journal of the Textile Institute* 101 (12):1035–49. doi:10.1080/00405000903205467.

Iooss, B., and C. Prieur. 2019. Shapley effects for sensitivity analysis with correlated inputs: Comparisons with Sobol'indices, numerical estimation and applications. *International Journal for Uncertainty Quantification* 9 (5):493–514. doi:10.1615/Int.J.UncertaintyQuantification.2019028372.

Jelil, R. A. 2015. A review of low-temperature plasma treatment of textile materials. *Journal of Materials Science* 50 (18):5913–43. doi:10.1007/s10853-015-9152-4.

Kan, C. W., H. F. Cheung, and Q. Chan. 2016. A study of plasma-induced ozone treatment on the colour fading of dyed cotton. *Journal of Cleaner Production* 112 (4):3514–24. doi:10.1016/j.jclepro.2015.10.100.

Kan, C. W., H. F. Cheung, and F. M. Kooh. 2017. An investigation of color fading of sulfur-dyed cotton fabric by plasma treatment. *Fibers and Polymers* 18 (4):767–72. doi:10.1007/s12221-017-6934-0.

Kayri, M. 2016. Predictive abilities of Bayesian regularization and Levenberg–Marquardt algorithms in artificial neural networks: A comparative empirical study on social data. *Mathematical and Computational Applications* 21 (2):20. doi:10.3390/mca21020020.

Liu, Y. H., C. K. M. To, M. K. Ngai, C. W. Kan, and H. Chua. 2019. Atmospheric pressure plasma-induced decolorisation of cotton knitted fabric dyed with reactive dye. *Coloration Technology* 135 (6):516–28. doi:10.1111/cote.12441.

Minaker, S. A., R. H. Mason, and D. R. Chow. 2021. Optimizing color performance of the ngenuity 3-dimensional visualization system. *Ophthalmology Science* 1 (3):1–9. doi:10.1016/j.xops.2021.100054.

Mitrović, T., M. Ristić, A. Perić Grujić, and S. Lazović. 2020. ANN prediction of the efficiency of the decolourisation of organic dyes in wastewater by plasma needle. *Journal of the Serbian Chemical Society* 85 (6):831–44. doi:10.2298/JSC191004002M.

Omerogullari Basyigit, Z., C. Eyupoglu, S. Eyupoglu, and N. Merdan. 2023. Investigation and feed-forward neural network-based estimation of dyeing properties of air plasma treated wool fabric dyed with natural dye obtained from Hibiscus Sabdariffa. *Coloration Technology* 1–13. doi:10.1111/cote.12665.

Ostertagova, E., and O. Ostertag. 2012. Forecasting using simple exponential smoothing method. *Acta Electrotechnica et Informatica* 12 (3):62–66. doi:10.2478/v10198-012-0034-2.

Özkan, İ., P. D. Baykal, and H. Özdemir. 2018. Effects of intermingled yarn surface characteristics on knitted fabric's color parameters. *Tekstil ve Mühendis* 25 (112):327–34. doi:10.7216/1300759920182511206.

Paul, R. 2015. Denim and jeans: an overview. In *Denim*, ed. R. Paul, 1–11. United Kingdom: Woodhead Publishing.

Peran, J., and S. Ercegović Ražić. 2020. Application of atmospheric pressure plasma technology for textile surface modification. *Textile Research Journal* 90 (9–10):1174–97. doi:10.1177/0040517519883954.

Rodriguez, J. D., A. Perez, and J. A. Lozano. 2009. Sensitivity analysis of k-fold cross validation in prediction error estimation. *IEEE Transactions on Pattern Analysis & Machine Intelligence* 32 (3):569–75. doi:10.1109/TPAMI.2009.187.

Samanta, K., S. Basak, and S. Chattopadhyay. 2017. Environmentally friendly denim processing using water-free technologies. In *Sustainability in denim*, ed. K. Samanta, S. Basak, and S. Chattopadhyay, 319–48. United Kingdom: Woodhead Publishing.

Shaffer, K. J., T. M. McLean, M. R. Waterland, M. Wenzel, and P. G. Plieger. 2012. Structural characterisation of difluoro-boron chelates of quino [7, 8-h] quinoline. *Inorganica chimica acta* 380:278–83. doi:10.1016/j.ica.2011.09.046.

Srikrishnan, M., and S. Jyoshitaa. 2022. An overview of preparation, processes for sustainable denim manufacturing. In *Sustainable approaches in textiles and fashion*, ed. S. M. Subramanian, 119–31. Singapore: Springer.

Tang, A. Y. L., C. H. Lee, Y. Wang, and C. W. Kan. 2018. Dyeing properties of cotton with reactive dye in nonane nonaqueous reverse micelle system. *ACS Omega* 3 (3):2812–19. doi:10.1021/acsomega.8b00032.

Yadav, S., and S. Shukla. 2016. Analysis of k-fold cross-validation over hold-out validation on colossal datasets for quality classification. 2016 IEEE 6th International Advance Computing Conference (IACC), Bhimavaram, India, Feb 27-28

Zhang, Y., and Y. Yang. 2015. Cross-validation for selecting a model selection procedure. *Journal of Econometrics* 187 (1):95–112. doi:10.1016/j.jeconom.2015.02.006.

Zhang, J., Z. Zheng, J. Zhang, and J. Li. 2008. "Low-Temperature Plasma-Induced Degradation of Aqueous 2, 4-Dinitrophenol." *Journal of Hazardous Materials* 154 (1–3): 506–512. doi:10.1016/j.jhazmat.2007.10.053.

Zille, A., F. R. Oliveira, and A. P. Souto. 2015. Plasma treatment in textile industry. *Plasma Processes and Polymers* 12 (2):98–131. doi:10.1002/ppap.201400052.